Surface-Phase Junctions

DOI: 10.1002/anie.200704788

Importance of the Relationship between Surface Phases and Photocatalytic Activity of TiO_2**

*Jing Zhang, Qian Xu, Zhaochi Feng, Meijun Li, and Can Li**

Semiconductor photocatalysts have attracted much research attention in the past decades owing to their applications to environmental purification and solar energy conversion.[1] Among photocatalysts, TiO_2 appears to be the most promising and suitable material because of its superior photocatalytic activity, chemical stability, low cost, and nontoxicity. The most significant factor that influences the photocatalytic performance of TiO_2 is its crystal form.[2] Two major crystalline phases of TiO_2, anatase and rutile, are commonly used in photocatalytic reactions.[3]

The surface phase of TiO_2, which is directly exposed to light and the reactants, contributes to photocatalysis and solar energy conversion because the photocatalytic reaction or photoelectron conversion takes place only when photoinduced electrons and holes are available on the surface.[4,5] The crystalline phase of TiO_2 particles in the surface region may be different from that in the bulk region,[6,7] particularly when TiO_2 is in its transition stage of the phase transformation from anatase to rutile.[7] Accordingly, a direct correlation between the surface phases of TiO_2 and its photocatalytic performance is of great significance, but has remained unclear mainly owing to the difficulty in characterizing the surface phase of TiO_2, especially of TiO_2 nanoparticles, which have been applied as catalysts or photocatalysts.

Herein, the surface phase of TiO_2 is differentiated by UV Raman spectroscopy combined with XRD, visible Raman spectroscopy, and high-resolution TEM (HRTEM). The photocatalytic activity of TiO_2 is found to be directly related to its surface phase. On the basis of the understanding thus obtained, we found that the photocatalytic activity of TiO_2 can be enhanced up to four times when anatase nanoparticles are deposited on the surface of rutile particles.

[*] Dr. J. Zhang, Q. Xu, Z. Feng, M. Li, Prof. Dr. C. Li
State Key Laboratory of Catalysis
Dalian Institute of Chemical Physics
Chinese Academy of Sciences
457 Zhongshan Road, Dalian 116023 (China)
Fax: (+86) 411-8469-4447
http://www.canli.dicp.ac.cn
E-mail: canli@dicp.ac.cn

[**] This work was supported by the National Natural Science Foundation of China (NSFC, Grant No. 20673112), the National Basic Research Program of China (Grant Nos. 2003CB615806 and 2003CB214504), and the Knowledge Innovation Program of the Chinese Academy of Sciences (Grant No. DICP K2006E2). We thank Fengtao Fan for help with the illustrations and Zili Wu for discussions.

Supporting information for this article is available on the WWW under http://www.angewandte.org or from the author.

TiO_2 samples with different bulk and surface crystalline phases were prepared by calcining $Ti(OH)_4$ in air from 500 to 800 °C.[7] Upon increasing the calcination temperature or calcination time, the anatase TiO_2 transforms gradually to the rutile phase. According to the results of XRD, as well as visible and UV Raman spectroscopy (Figure S1 in the Supporting Information), both the surface and bulk regions of the TiO_2 sample calcined at 500 °C are in the pure anatase form. The anatase phase in the bulk begins to transform into the rutile phase at only 550 °C, while the surface region maintains the anatase phase when the calcination temperature is below 680 °C. Upon further increasing the calcination temperature to 700 °C or above, almost all bulk TiO_2 is converted into the rutile phase while about 44 % anatase phase still remains in the surface region. The anatase phase in the surface region is completely transformed into the rutile phase only when the calcination temperature is increased up to 800 °C.

The rutile content in the bulk region and the anatase content in the surface region, estimated from visible and UV Raman spectra, are shown by the solid and broken curves, respectively, in Figure 1a. Figure 1b shows the rate of H_2 production from the photocatalytic reaction of water and methanol over TiO_2 (deposited with Pt as cocatalyst) that has been calcined at different temperatures. The process of the phase transformation of TiO_2 from anatase to rutile[7] is schematically shown in Figure 1b.

The rate of H_2 evolution does not evidently change for the TiO_2 calcined from 500 to 680 °C, although the amount of the rutile phase in the bulk region is greatly increased (Figure 1b). It is obvious that the overall photocatalytic activity is more directly related to its surface phase because the anatase phase always exists in the surface region for the samples calcined at 500–680 °C. A maximum activity is observed for TiO_2 samples calcined at 700–750 °C, whereby the bulk of TiO_2 is almost in the pure rutile phase while the surface is in a mixed phase of anatase and rutile. The anatase phase in the surface region of the TiO_2 sample is completely transformed into the rutile phase when the calcination temperature is increased to 800 °C, and correspondingly the overall photocatalytic activity decreases dramatically. Thus, the pure rutile phase shows low overall activity for H_2 production. This result suggests that the presence of the surface anatase on rutile TiO_2 can keep a relatively high overall photocatalytic activity.

To explore the intrinsic photoactivity of the TiO_2 sample calcined at different temperatures, the surface specific activity, that is, the amount of H_2 production per surface area ($\mu mol\,h^{-1}\,m^{-2}$), of the samples calcined at different temperatures is compared in Figure 1c (the specific surface area of the TiO_2 sample calcined at different temperatures is

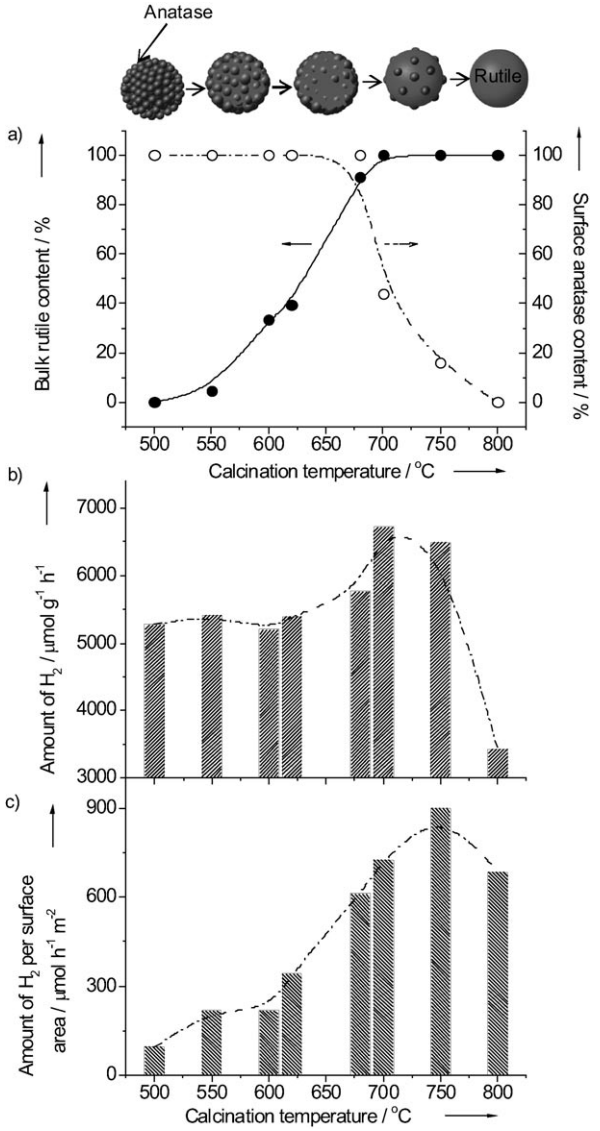

Figure 1. a) Dependence of bulk rutile content (filled circles, solid line) and surface anatase content (open circles, broken line) on the calcination temperature. b,c) TiO_2 samples calcined at different temperatures and their corresponding overall (b) and surface-specific photocatalytic activity (c).

given in Table S1 in the Supporting Information). The surface specific activity increases with increasing the calcination temperature, and it reaches a maximum at 700–750 °C.

It is very interesting to note in Figure 1 b,c that the TiO_2 samples calcined at 700–750 °C exhibit the highest photocatalytic activities (for both overall and surface specific activity). UV Raman spectra of these samples indicate that the mixed phases of anatase and rutile coexist in the surface region. Namely, when the TiO_2 sample is calcined at 700–750 °C, the phase junctions between anatase and rutile are derived on the surface of the rutile TiO_2, as characterized by UV Raman spectroscopy combined with XRD and visible Raman spectroscopy (Figure S1 in the Supporting Information).

The formation of the surface-phase junction could promote the spatial charge separation[8–10] in the surface region; in other words, the formation of the surface-phase junctions between the anatase nanoparticles and rutile particles may be responsible for the highest photocatalytic activity of the sample calcined at 700–750 °C. The phase junctions may facilitate transfer of the photogenerated electron from the conduction band of the rutile phase to the trapping sites on the anatase surface,[11,12] thereby improving the charge-separation efficiency and enhancing the photocatalytic activity. To further confirm the surface-phase effect of TiO_2, the overall and specific photocatalytic activities of TiO_2 samples that were calcined at 600 °C for different periods of time were investigated because the surface-phase composition in the TiO_2 sample can be carefully controlled by calcination at 600 °C for different time periods (Figure S2 in the Supporting Information).

To further demonstrate that higher photocatalytic activity can be achieved for a TiO_2 photocatalyst with a surface junction formed between anatase and rutile TiO_2, anatase TiO_2 nanoparticles were deposited on rutile TiO_2 particles by a wet-impregnation method,[13] and then the TiO_2 powder was calcined up to 400 °C to convert the deposited TiO_2 on the rutile surface into the anatase phase while keeping the bulk still in the rutile phase. To obtain the samples with different amounts of anatase phase on the surface of the rutile TiO_2 particles, the impregnation procedure was repeated (the loading of anatase deposited on the surface of the rutile particles was roughly 5 wt % for each time). The as-prepared samples are denoted as TiO_2(A)/TiO_2(R)-*n*, in which TiO_2(A) indicates the surface anatase TiO_2 nanoparticle, TiO_2(R) indicates the rutile TiO_2 particle as the support, and *n* indicates the number of impregnation processes. Figure 2 a–c shows the SEM images of TiO_2(A)/TiO_2(R)-0, -1, and -4 samples, in which it is clearly observed that fine anatase particles (particle size < 30 nm) are highly dispersed on the rutile particles (particle size ca. 500 nm) in the TiO_2(A)/TiO_2(R)-*n* samples.

The surface specific activity of TiO_2(A)/TiO_2(R) catalysts with increasing amount of anatase on the surface of rutile are given in Figure 2 d. The anatase content estimated from XRD and UV Raman spectroscopy is also displayed in Figure 2 d (XRD and UV Raman spectra are shown in Figure S3 in the Supporting Information). Compared with the pure rutile TiO_2 support, the photocatalytic activity is remarkably increased by supporting a small amount of anatase on the surface of rutile TiO_2. For example, TiO_2(A)/TiO_2(R)-1 and -2 samples exhibit much higher photocatalytic activities despite their low surface anatase content (< 10 wt %); for TiO_2(A)/TiO_2(R)-3, the photocatalytic activity is greatly enhanced to about four times higher than that of pure rutile TiO_2. This enormous increase in the photocatalytic activity can be attributed to the formation of the surface anatase/rutile phase junction. For the TiO_2(A)/TiO_2(R)-4 sample, the photocatalytic activity is decreased somewhat because the surface of the rutile TiO_2 may be fully covered by the anatase nanoparticles, which decreases the amount of exposed anatase/rutile phase junction on the TiO_2 surface.

To visualize the surface-phase junction, the TiO_2 (A)/TiO_2 (R)-*n* ($n = 1$–4) samples were investigated by HRTEM. Figure 3 shows the HRTEM results of the TiO_2(A)/

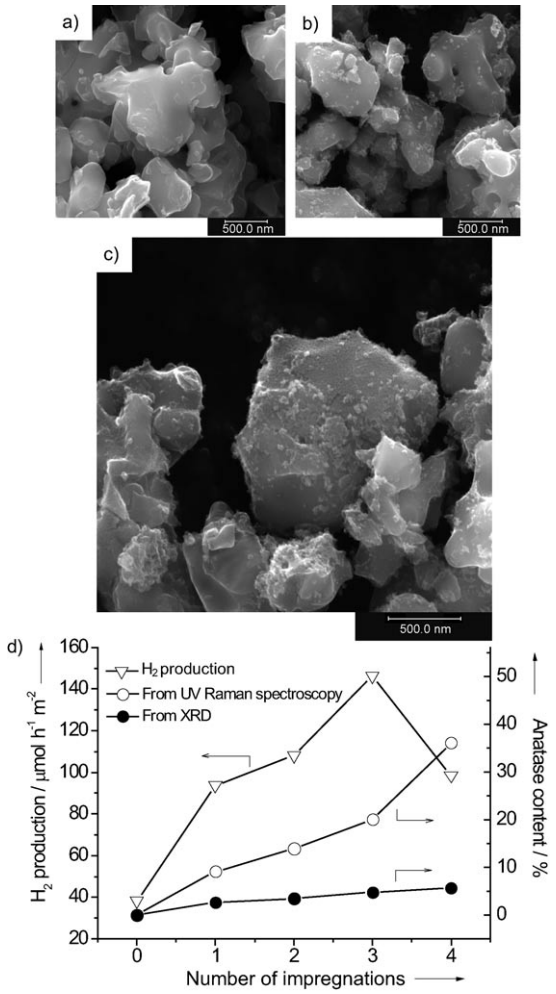

Figure 2. Scanning electron micrographs of a) TiO_2(R), b) TiO_2(A)/TiO_2(R)-1, and c) TiO_2(A)/TiO_2(R)-4. d) The photocatalytic activities for evolved H_2 per surface area of TiO_2(A)/TiO_2(R)-*n* samples with increasing amount of anatase phase on the surface of rutile TiO_2. The rate of evolved H_2 per surface area of TiO_2(R) before depositing anatase TiO_2 is added for comparison (data point at 0 impregnations). The anatase contents estimated from XRD and UV Raman spctroscopy for TiO_2(A)/TiO_2(R)-*n* samples are also displayed.

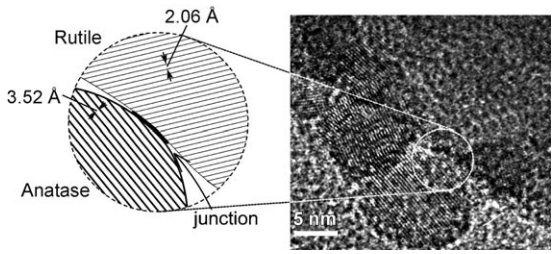

Figure 3. HRTEM image of a TiO_2(A)/TiO_2(R)-*n* sample.

TiO_2(R)-*n* samples and clearly shows that the junction structure between the anatase and rutile phase is formed in TiO_2(A)/TiO_2(R)-*n*. HRTEM gives the direct evidence for the surface anatase/rutile junction formed on rutile TiO_2 particles.

This work shows that the photocatalytic activity of TiO_2 nanoparticles is directly related to the surface-phase structure, which can be sensitively detected by UV Raman spectroscopy and can also be visualized by HRTEM. More interestingly, it is found that the phase junction formed between the surface anatase nanoparticles and rutile particles can greatly enhance the photocatalytic activity for photocatalytic H_2 production. From this work it can thus be concluded that the surface-phase junction of a semiconductor catalyst directly contributes to photocatalytic reactions and, therefore, provides a possible strategy to develop high-performance photocatalysts by designing and preparing the surface-phase junctions.

Experimental Section

Preparation of TiO_2(A)/TiO_2(R)-*n*: The rutile TiO_2 support (Alfa Aesar, 99.8% rutile phase), in single rutile phase confirmed by XRD, visible Raman, and UV Raman spectroscopy, was impregnated with a solution of titanium tetraisopropoxide in 2-propanol (the weight ratio of anatase phase to rutile phase in the parent solution 5 wt%), and subsequently treated for 8 h at 423 K in the presence of a flow of wet nitrogen to hydrolyze the titanium isopropoxide. After the impregnation, the TiO_2 powder was calcined up to 400 °C to convert the TiO_2 deposited on the rutile surface into the anatase phase while keeping the bulk in the rutile phase. To obtain samples with different amounts of anatase phase on the surface of rutile TiO_2 particles, the impregnation procedure was repeated.

Characterization: UV Raman spectra were recorded at room temperature with a Jobin–Yvon T64000 triple-stage spectrograph with a spectral resolution of 2 cm^{-1}. The laser line at 325 nm of a He–Cd laser was used as an excitation source with an output of 25 mW. The power of the laser at the sample was about 3.0 mW. Visible Raman spectra were recorded on a Jobin–Yvon U1000 scanning double monochromator with a spectral resolution of 4 cm^{-1}. The line at 532 nm from a DPSS 532 Model 200 532-nm single-frequency laser was used as the excitation source. XRD patterns were obtained on a Rigaku MiniFlex diffractometer with a $Cu_{K\alpha}$ radiation source. Diffraction patterns were collected from 20 to 80° at a speed of 5° min^{-1}. The morphology was examined with SEM QUANTA 200F. HRTEM images were obtained on a Tecnai G^2 F30 S-Twin (FEI company).

The photocatalytic H_2 evolution from methanol/water solutions was investigated over Pt-loaded TiO_2 samples. The photocatalytic reaction was carried out in a pyrex reaction cell connected to a closed gas circulation and evacuation system. The light source was a 300-W Xe lamp covered with a water-cooled quartz jacket. The TiO_2 photocatalyst (0.2 g) was suspended in an aqueous solution containing H_2O (160 mL) and CH_3OH (40 mL). Pt (0.3 wt%) was photodeposited on the TiO_2 catalysts in situ from precursor $H_2PtCl_6 \cdot 6H_2O$ under irradiation. The amount of H_2 was measured using on-line gas chromatography.

Received: October 16, 2007
Published online: January 22, 2008

Keywords: hydrogen generation · phase transitions · photocatalysis · titanium dioxide · UV Raman spectroscopy

[1] a) M. Grätzel, *Nature* **2001**, *414*, 338–344; b) M. A. Fox, M. T. Dulay, *Chem. Rev.* **1993**, *93*, 341–357; c) R. Wang, K. Hashimoto, A. Fujishima, M. Chikuni, E. Kojima, A. Kitamura, M.

Shimohigoshi, T. Watanabe, *Nature* **1997**, *388*, 431 – 432; d) P. V. Kamat, *Chem. Rev.* **1993**, *93*, 267 – 300.
[2] a) K. E. Karakitsou, X. E. Verykios, *J. Phys. Chem.* **1993**, *97*, 1184 – 1189; b) H. Tada, M. Tanaka, *Langmuir* **1997**, *13*, 360 – 364; c) A. P. Rivera, K. Tanaka, T. Hisanaga, *Appl. Catal. B* **1993**, *3*, 37 – 44; d) Z. Ding, G. Q. Lu, P. F. Greenfield, *J. Phys. Chem. B* **2000**, *104*, 4815 – 4820; e) J. F. Zhu, W. Zheng, B. He, J. L. Zhang, M. Anpo, *J. Mol. Catal. A* **2004**, *216*, 35 – 43.
[3] a) O. Carp, C. L. Huisman, A. Reller, *Prog. Solid State Chem.* **2004**, *32*, 33 – 177; b) J. Augustynski, *Electrochim. Acta* **1993**, *38*, 43 – 46.
[4] A. L. Linsebigler, G. Q. Lu, J. T. Yates, Jr., *Chem. Rev.* **1995**, *95*, 735 – 758.
[5] S. Sakthivel, M. C. Hidalgo, D. W. Bahnermann, S.-U. Geissen, V. Murugesan, A. Vogelpohl, *Appl. Catal. B* **2006**, *63*, 31 – 40.
[6] a) G. Busca, H. Saussey, O. Saur, J. C. Lavalley, V. Lorenzelli, *Appl. Catal.* **1985**, *14*, 245 – 260; b) G. Busca, G. Ramis, J. M. G. Amores, V. S. Escribano, P. Piaggio, *J. Chem. Soc. Faraday Trans.* **1994**, *90*, 3181 – 3190.
[7] J. Zhang, M. J. Li, Z. C. Feng, J. Chen, C. Li, *J. Phys. Chem. B* **2006**, *110*, 927 – 935.
[8] T. Ozawa, M. Iwasaki, H. Taka, T. Akita, K. Tanaka, S. Ito, *J. Colloid Interface Sci.* **2005**, *281*, 510 – 513.
[9] T. Kawahara, T. Ozawa, M. Iwasaki, H. Tada, S. Ito, *J. Colloid Interface Sci.* **2003**, *267*, 377 – 381.
[10] T. Kawahara, Y. Konishi, H. Tada, N. Tohge, J. Nishii, S. Ito, *Angew. Chem.* **2002**, *114*, 2935 – 2937; *Angew. Chem. Int. Ed.* **2002**, *41*, 2811 – 2813.
[11] T. Ohno, K. Tokieda, S. Higashida, M. Matsumura, *Appl. Catal. A* **2003**, *244*, 383 – 391.
[12] a) D. C. Hurum, K. A. Gray, T. Rajh, M. C. Thurnauer, *J. Phys. Chem. B* **2005**, *109*, 977 – 980; b) D. C. Hurum, A. G. Agrios, K. A. Gray, T. Rajh, M. C. Thurnauer, *J. Phys. Chem. B* **2003**, *107*, 4545 – 4549.
[13] V. Loddo, G. Marcì, C. Martín, L. Palmisano, V. Rives, A. Sclafani, *Appl. Catal. B* **1999**, *20*, 29 – 45.

